



Title	Silicon Nitride Joining with Silicate Glass Solder (I)(Materials, Metallurgy & Weldability)
Author(s)	Iwamoto, Nobuya; Umesaki, Norimasa; Haibara, Yukio
Citation	Transactions of JWRI. 1986, 15(2), p. 265-271
Version Type	VoR
URL	<a href="https://doi.org/10.18910/9987">https://doi.org/10.18910/9987</a>
rights	
Note	

*The University of Osaka Institutional Knowledge Archive : OUKA*

<https://ir.library.osaka-u.ac.jp/>

The University of Osaka

# Silicon Nitride Joining with Silicate Glass Solder (I)

Nobuya IWAMOTO\*, Norimasa UMESAKI\*\* and Yukio HAIBARA\*\*\*

## Abstract

*$\text{Si}_3\text{N}_4$ - $\text{Si}_3\text{N}_4$  joining was accomplished by the use of  $\text{CaO-SiO}_2\text{-TiO}_2$  glass solder without using applied pressure. The properties of the glasses used and the  $\text{Si}_3\text{N}_4$ -glass joining reactions were studied in detail. The strong bond strength obtained from  $\text{Si}_3\text{N}_4$  joints can be put to practical use.*

KEY WORDS: ( $\text{Si}_3\text{N}_4$ ) (Joining) (Glass Solder) ( $\text{CaO-SiO}_2\text{-TiO}_2$  System) (Microstructure) (Bond Strength)

## 1. Introduction

Silicon nitride ceramics are excellent for heat-, corrosion-, abrasion- and insulation-resistance, so these ceramics are being widely considered as materials for components in energy-conversion machines such as heat engines. Therefore, for the purpose of forming complex shapes, the joining of  $\text{Si}_3\text{N}_4$  is a useful and often necessary processing step. In general, joining processes have used wetting by a viscous interfacial phase or sintering/reaction of a powder layer with the solid components to form a bond.<sup>1)</sup> Both ways involve the use of applied pressure. The sealing technique with various oxide glass solders is being used to join ceramics and/or metals. It is well known that  $\text{Si}_3\text{N}_4$  is dissolved in oxide glass and that silicon oxynitride glass is consequently formed.<sup>2)</sup> This knowledge is now being more effectively applied to the joining of  $\text{Si}_3\text{N}_4$  ceramics. Recently, a method of joining  $\text{Si}_3\text{N}_4$  with oxide glasses was developed.<sup>3)-7)</sup> This technique consists of heating a thin layer of glass between the parts to be joined at a temperature and pressure sufficient to reach the molten glass  $\text{Si}_3\text{N}_4$  ceramics, thus creating the bond.<sup>6)</sup>

It is well known that the titanium element easily generates nitridation reactions under a nitrogen atmosphere. We have succeeded in getting a strong bond strength of  $\text{Si}_3\text{N}_4$ - $\text{Si}_3\text{N}_4$  ceramic joints at room-temperature by using  $\text{CaO-SiO}_2\text{-TiO}_2$  glass solder with nearly eutectic composition without using applied pressure. The results obtained are reported in this paper. In addition, the purpose of the present research was to understand the joining mechanism that took place between  $\text{Si}_3\text{N}_4$  and  $\text{CaO-SiO}_2\text{-TiO}_2$  glass solder in detail.

## 2. Experimental Procedure

### 2.1 Joining materials and process

A single type of sintered  $\text{Si}_3\text{N}_4$  ( $\beta$ - $\text{Si}_3\text{N}_4$ , Sumitomo Cement Co., Densification aid components:  $\text{MgO}$ ,  $\text{Al}_2\text{O}_3$ ,  $\text{Y}_2\text{O}_3$ ) was used in this study. Each material was cut into plates of approximately  $15 \times 30 \times 15$  mm or  $10 \times 10 \times 20$  mm using a diamond cutter, and was then ground using #600 diamond wheels to produce a flat surface ( $6.5 \mu\text{m R}_{\max}$  L0.8).

The  $\text{CaO-SiO}_2\text{-TiO}_2$  glasses with nearly eutectic composition ( $25\text{wt\%} \leq \text{CaO} \leq 65\text{wt\%}$ ,  $15\text{wt\%} \leq \text{SiO}_2 \leq 65\text{wt\%}$ ,  $0\text{wt\%} \leq \text{TiO}_2 \leq 65\text{wt\%}$ ) were prepared by melting suitable mixtures of analytical grade reagents  $\text{CaCO}_3$ ,  $\text{SiO}_2$  and  $\text{TiO}_2$  for 30 to 60 min in air  $1500^\circ$  to  $1550^\circ\text{C}$  in a Pt crucible under an electric furnace. In order to make glass samples, the melts were quenched by dipping the Pt crucible partially in cold water. The glass samples obtained were ground to a fine powder using an  $\text{Al}_2\text{O}_3$  mortar and pestle for further experiments.

The glass samples were characterized by a variety of property measurement technique. Laser Raman spectra were measured on a JASCO model R-800 double-grating spectrometer at a scattering angle of  $90^\circ$ . The excitation source was the  $514.5 \text{ nm}$  ( $19435.6 \text{ cm}^{-1}$ ) line of a NEC GLG-3300 Ar ion laser at a power of from 300 to 400 mW. The glass transition temperature ( $T_g$ ), the softening temperature ( $T_s$ ), the crystallization temperature ( $T_c$ ) and the temperature of the melting point ( $T_m$ ) were measured in a DTA apparatus with  $\text{Al}_2\text{O}_3$  as the reference. After DTA measurement, an X-ray diffraction experiment was performed on the crystallized samples. The expansion

\* Received on November 1, 1986

† Professor

\*\* Research Instructor

\*\*\* Central Research Laboratory, Sumitomo Cement Co., Ltd.

Transactions of JWRI is published by Welding Research Institute of Osaka University, Ibaraki, Osaka 567, Japan

was measured by using fused  $\text{SiO}_2$  as a standard.

Fig. 1 indicates the outline of a  $\text{Si}_3\text{N}_4$  joining process developed by use. Glass paste mixed with screen oil was painted on one side of the surface of each  $\text{Si}_3\text{N}_4$  plate. After drying, a sandwich of glass solder was put between  $\text{Si}_3\text{N}_4$  plates, and then  $\text{Si}_3\text{N}_4$  joining was carried out by heating for 10 to 30 min at 1400° to 1600°C under various atmospheres ( $\text{N}_2$ , Ar,  $\text{N}_2$  of 5 kg/cm<sup>2</sup>, 5 $\text{H}_2$ /95 $\text{N}_2$ , air and a vacuum of  $5 \times 10^{-3}$  torr). No external pressure was used in joining the two plates.

## 2.2 Microstructural analysis

The joint cross section produced were metallographically polished and then observed by means of an optical microscope, EPMA and SEM-EDX. Slices of the typical joint cross sections were ground, polished, and then Ar-ion-thinned to prepare electron-transparent samples for TEM observation. The transmission electron microscope (AEM) was performed on a HITACHI H800 200 kV TEM-EDX. A few joint regions were examined analysis (Beam diameter: 100 $\mu\text{m}\phi$ ).

## 2.3 Bond strength test

The joint plates were cut into test bars of approximately 5 × 4 × 60 mm or 3 × 3 × 60 mm with the plane of the joint in the center of the test bar. The bond strength of each joint was measured by a four-point bending machine with a span length of 30 mm using a loading rate of 0.5 mm/min.

## 3. Results and Discussion

### 3.1 Properties of the glass solder

Fig. 2 shows the Raman spectrum of a typical 30wt%CaO-35wt% $\text{SiO}_2$ -35wt% $\text{TiO}_2$  glass. As shown in this figure, the weak Raman bands in the frequency range from about 800 to 1200 cm<sup>-1</sup> are due to the Si-O stretching vibration of depolymerized silicate anions such as the  $\text{Si}_2\text{O}_5^{2-}$  sheet, the  $\text{SiO}_3^{2-}$  chain, the  $\text{Si}_2\text{O}_7^{6-}$  dimer and the  $\text{SiO}_4^{4-}$  monomer.<sup>8)</sup> This result implies a relatively low viscosity of the glasses in the molten state and thus good wetting between the molten glasses and  $\text{Si}_3\text{N}_4$  in the joining process. Furthermore, the Raman spectrum obtained suggests that  $\text{Ti}^{4+}$  ions with four-fold oxygen coordination ( $\text{TiO}_4$  tetrahedron) and six-fold oxygen coordination ( $\text{TiO}_6$  octahedron) may coexist in the glass.

Fig. 3 shows the DTA curve of 30wt%CaO-35wt% $\text{SiO}_2$ -35wt% $\text{TiO}_2$  glass for the temperature interval between room-temperature and 1400°C. The glass transition temperature  $T_g$  (= 750°C) and the glass softening temperature  $T_s$  (= 770°C) were observed by this DTA measurement. As shown in this figure, there were exothermic

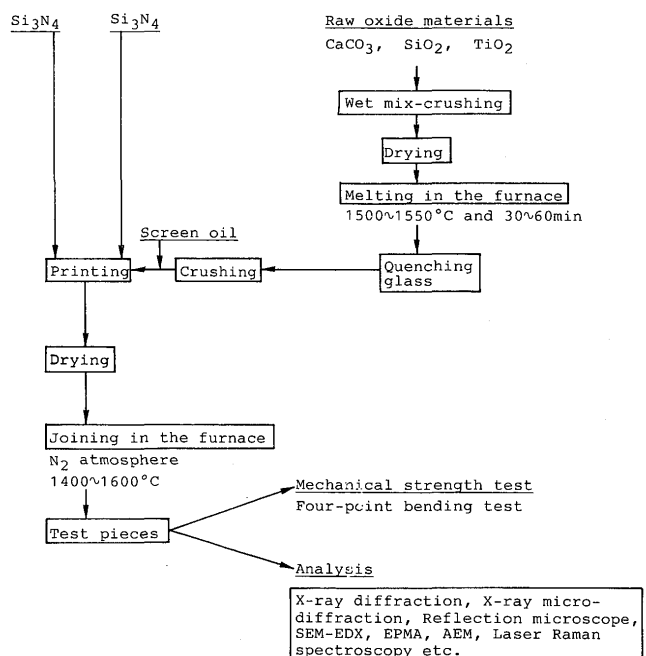


Fig. 1 Process of  $\text{Si}_3\text{N}_4$  joining.

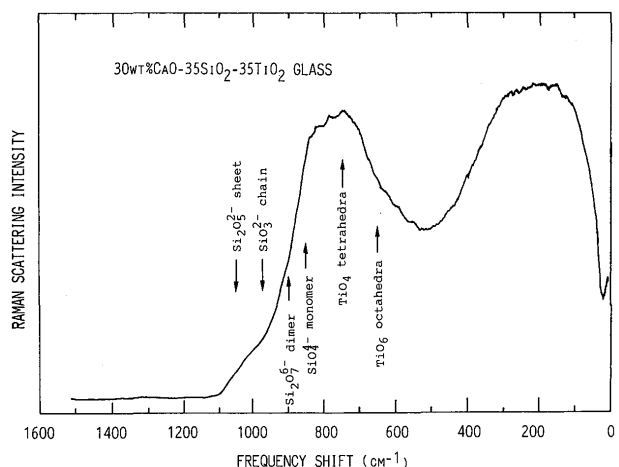


Fig. 2 Raman spectrum of 30wt%CaO-35wt% $\text{SiO}_2$ -35wt% $\text{TiO}_2$  glass.

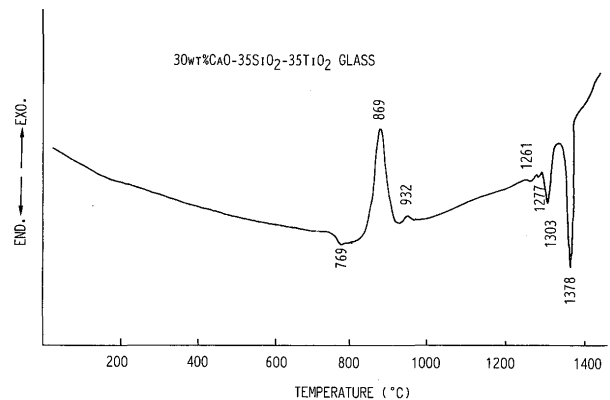


Fig. 3 DTA curve of 30wt%CaO-35wt% $\text{SiO}_2$ -35wt% $\text{TiO}_2$  glass.

peaks at  $T_c$  = 870°C and 940°C due to crystallization, and then four endothermic peaks at  $T_m$  = 1261° to 1378°C

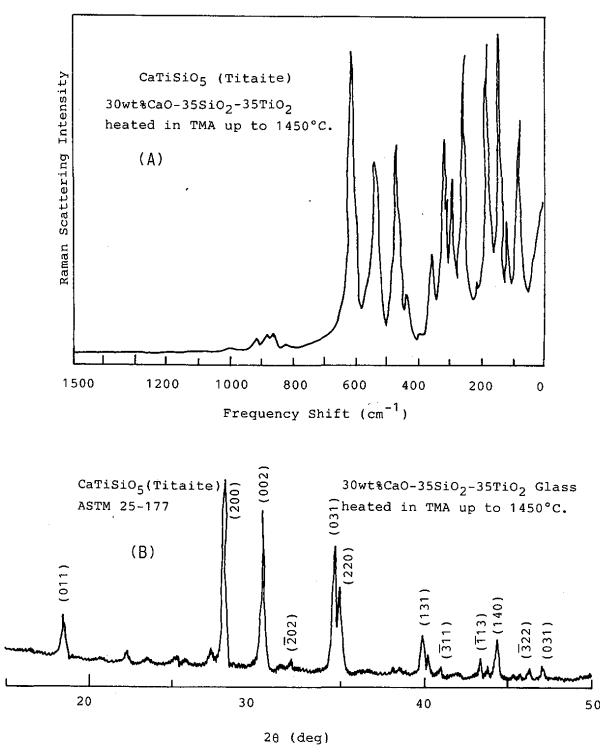


Fig. 4 Raman spectrum (A) and X-ray diffraction pattern (B) of 30wt%CaO-35wt%SiO<sub>2</sub>-35wt%TiO<sub>2</sub> glass crystallized by the DTA test.

due to melting. After DTA measurement, the CaTiSiO<sub>5</sub> titanite phase crystallized from the glass was confirmed by Raman spectroscopy and X-ray diffraction (see Fig. 4).

Fig. 5 shows the thermal expansion curve of 30wt% CaO-35wt%SiO<sub>2</sub>-35wt%TiO<sub>2</sub> glass. The thermal expansion coefficient for the temperature interval between room-temperature and 628°C was found to be  $\alpha_g = 1.29 \times 10^{-6}/\text{°C}$ . This value is about 1/3 that of the Si<sub>3</sub>N<sub>4</sub> ( $\alpha_c = 2.8 \sim 3.0 \times 10^{-6}/\text{°C}$ ) used, and compressive stress between the Si<sub>3</sub>N<sub>4</sub> and the glass is consequently produced. Johnson and Rowcliffe<sup>7)</sup> reported that the difference in the thermal expansion coefficients between

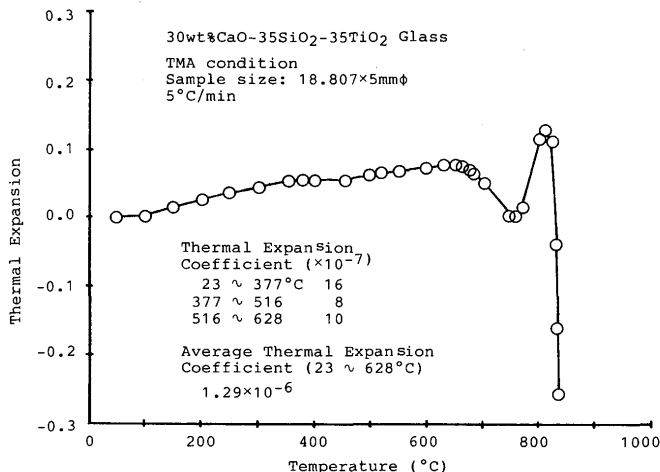


Fig. 5 Thermal expansion curve of 30wt%CaO-35wt%SiO<sub>2</sub>-35wt%TiO<sub>2</sub> glass.

Si<sub>3</sub>N<sub>4</sub> and glass can cause thermal fracture as a result of the mismatch. As opposed to the glasses used by them<sup>7)</sup> is almost double that of hot-pressed Si<sub>3</sub>N<sub>4</sub>,<sup>7)</sup> and tensile stress between the Si<sub>3</sub>N<sub>4</sub> and the glass is consequently produced. It seems that tensile stress develops thereby causing thermal expansion cracks.

### 3.2 Si<sub>3</sub>N<sub>4</sub>-glass reactions

Si<sub>3</sub>N<sub>4</sub> joined with 35wt%CaO-40wt%SiO<sub>2</sub>-25wt%TiO<sub>2</sub> glass at 1500°C for 30 min under N<sub>2</sub> gas at 5 kg/cm<sup>2</sup> gave a higher bond strength. The results obtained from the microstructural analysis regarding this Si<sub>3</sub>N<sub>4</sub> joint are described in this section.

Fig. 6 shows an optical micrograph of the joint region in the bonded Si<sub>3</sub>N<sub>4</sub>. This picture indicates the formation of the condensed joint region with a thickness of about 20μm. The joint is characterized by the golden thin-layer, which consists of titanium nitride (for details, please see below).

The EPMA micrographs of the joint region in the bonded Si<sub>3</sub>N<sub>4</sub> and the corresponding X-ray maps for selected elements Ti, N, Ca, O, Si, Al and Y are shown in Fig. 7. The X-ray map for the element Ti illustrates that the Ti is clearly distributed in the joint region, and does not diffuse into Si<sub>3</sub>N<sub>4</sub> throughout the molten glass. Because the distribution of the element Ti is almost in accord with that of the element N, the result indicates that the elements Ti and N form a titanium nitride compound. On

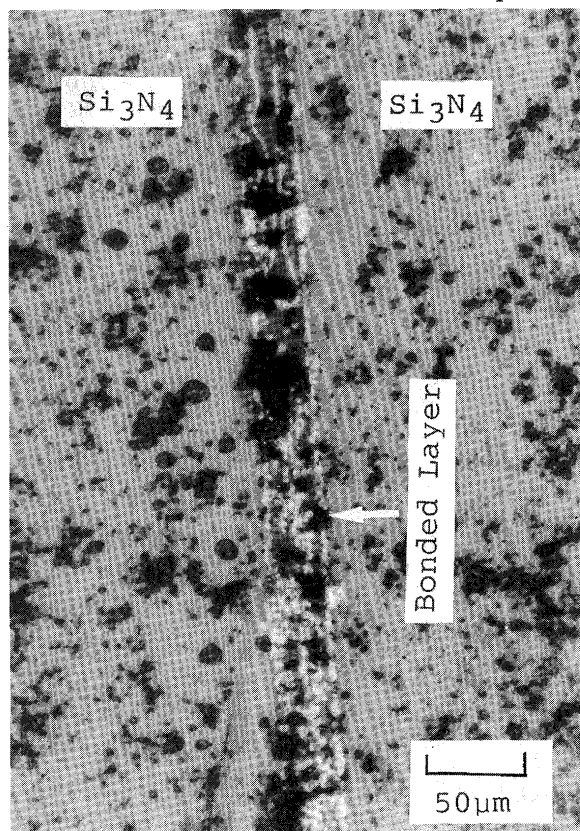


Fig. 6 Optical micrograph of joint region.

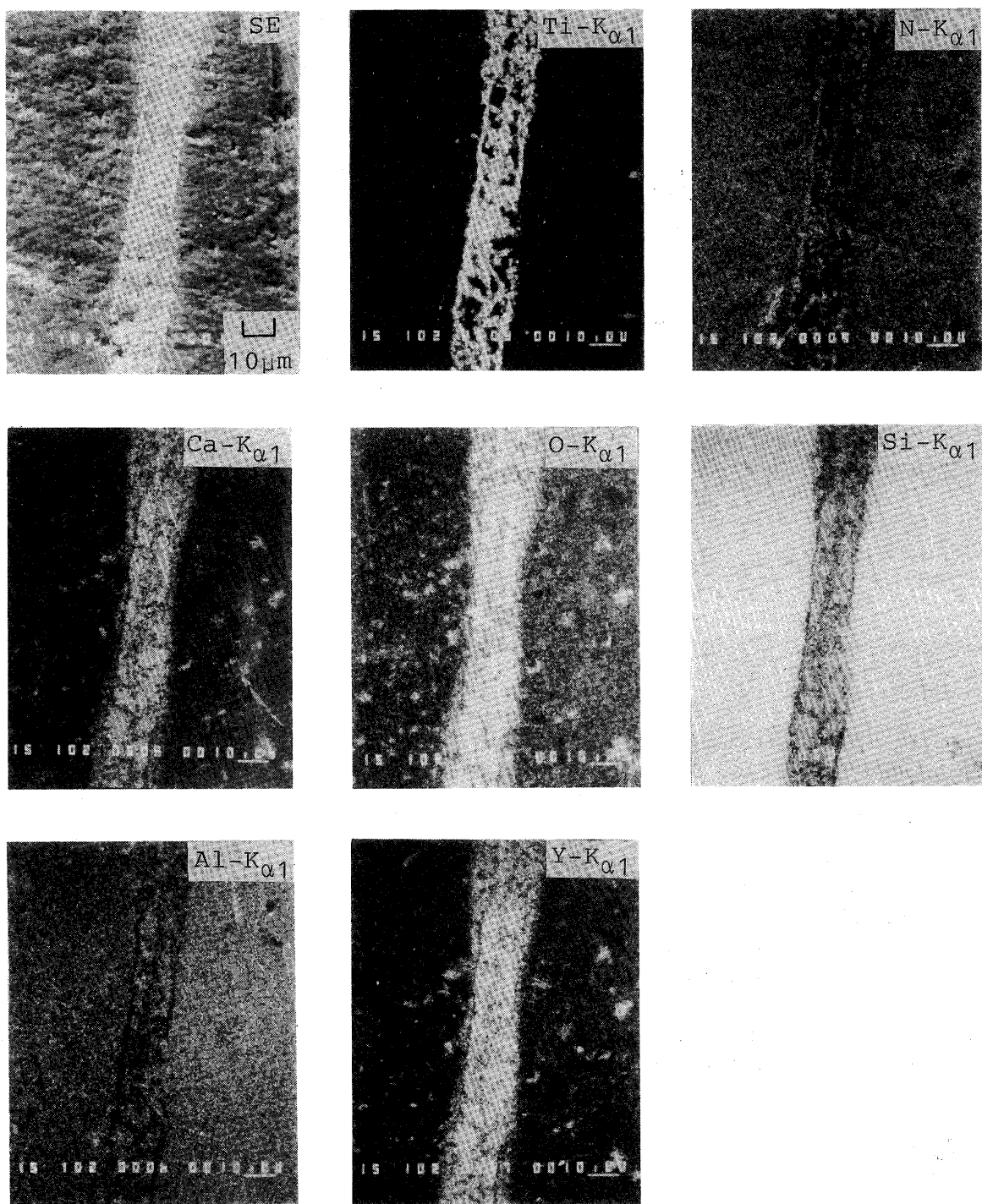


Fig. 7 EPMA micrographs of joint region in the bonded  $\text{Si}_3\text{N}_4$ .

the other hand, the X-ray maps for the elements Ca and O illustrate that the Ca and O are relatively distributed over all in the joint region, and the distribution of these elements extends for about  $2 \sim 3\mu\text{m}$  from the bonding interface to  $\text{Si}_3\text{N}_4$ . In addition, the elements Ca and O are slightly soluble in the Ti-rich nitride compound in the joint region, as can be seen in these pictures. As previously mentioned, the elements Al, Y and Mg are densification aid components for the  $\text{Si}_3\text{N}_4$  ceramics used. It is well known that these densification aid elements are present in

glassy joining phases between  $\beta\text{-Si}_3\text{N}_4$  grains. The fact that should be taken notice of is the behavior of Y in the joint region. The X-ray map for the element Y illustrates that Y diffuses from the  $\text{Si}_3\text{N}_4$  grain boundaries to the joint region during joining, and consequently is densely distributed over all into the joint region.

Fig. 8 shows the X-ray microdiffraction patterns of the joint region in the bonded  $\text{Si}_3\text{N}_4$ . As shown in Fig. 8 (A), the above-mentioned layer-like compound was identified as titanium nitride  $\text{TiN}$ . It can be considered that the

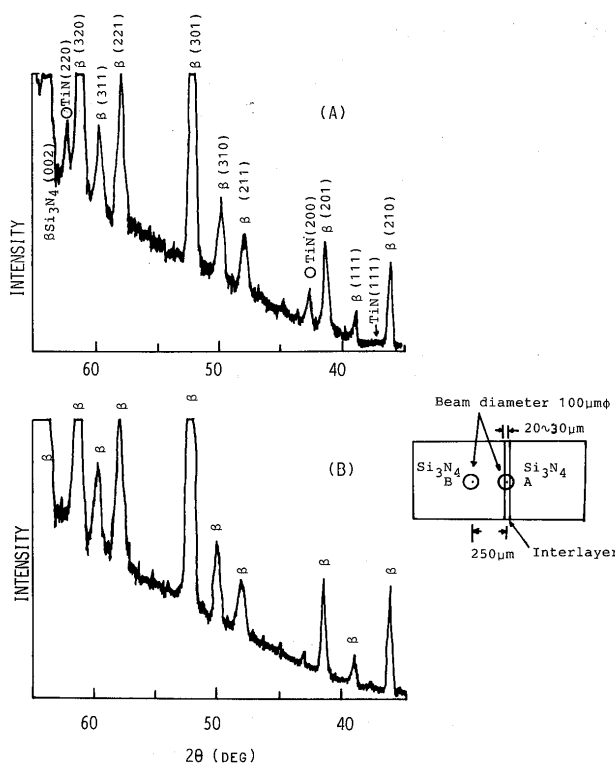
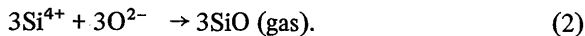
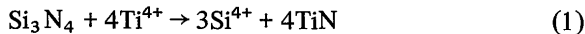


Fig. 8 X-ray microdiffraction patterns of joint region in the bonded  $\text{Si}_3\text{N}_4$ .

$\text{Si}_3\text{N}_4$  dissolves in the molten glass, and the titanium nitride precipitates as a result of the following reaction between the  $\text{Si}_3\text{N}_4$  and  $\text{Ti}^{4+}$  ions in the molten glass:



$\text{O}^{2-}$  is free oxygen existing in the molten glass. It is generally accepted that the introduction of oxides such as  $\text{CaO}$  and  $\text{TiO}_2$  to  $\text{SiO}_2$  melt breaks the Si-O-Si bridging bonds connecting  $\text{SiO}_4$  tetrahedra of three-dimensional network units, creating non-bridging ( $\text{O}^-$ ) and free ( $\text{O}^{2-}$ ) oxygen. No band for the (111) plane of the precipitated TiN (Crystal structure: NaCl type) appears in the obtained X-ray micro-diffraction pattern, as can be seen in Fig. 8 (A). This is caused by the distortion of the TiN crystalline structure due to other elements (O, Si, Al, Y, Ca and Mg) dissolved in TiN precipitates. The only identified crystalline species in the joint region are  $\beta$ - $\text{Si}_3\text{N}_4$  and TiN. Consequently, the joint consists of the layer-like TiN precipitates and glassy matrix.

Fig. 9 shows the SEM-EDX micrograph of the bonded  $\text{Si}_3\text{N}_4$ -glass interface. This picture reveals that there is a thin-layer based on Al-Si-Y-Ca-Ti between the  $\text{Si}_3\text{N}_4$  and the TiN precipitates. As previously mentioned, the layer region dissolves oxygen and nitrogen, and is of the glassy phase. It is, therefore, considered that the thin-layer consists of oxynitride glasses based on the Al-Si-Y-Ca-Ti

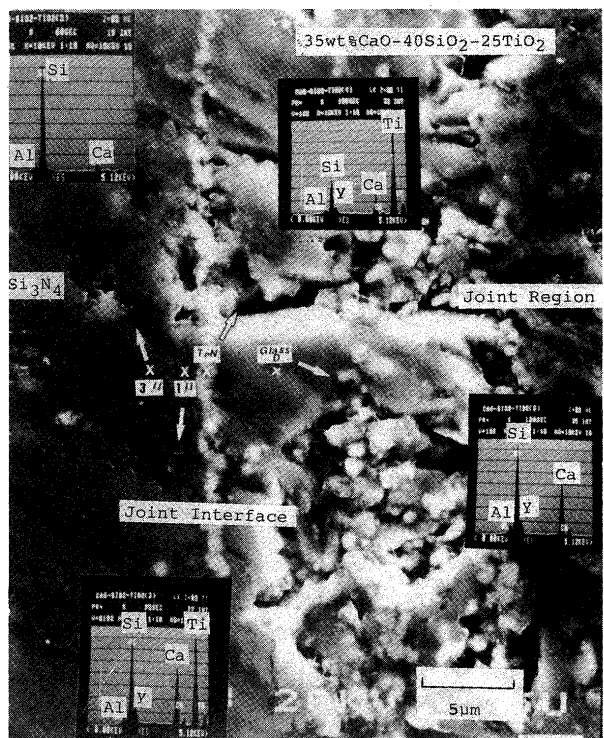


Fig. 9 SEM micrographs of joint region in the bonded  $\text{Si}_3\text{N}_4$ .

system. The presence of the glassy thin-layer probably makes it possible to accomplish our  $\text{Si}_3\text{N}_4$  joining.

Fig. 10 shows the transmission micrograph of the oxynitride glassy layer existing in the bonded interface found by SEM-EDX observation. As shown in this picture, the microstructure is characteristic of the intergranular phase and the boundary phase. The electron diffraction patterns obtained from both phases indicate the diffuse rings due to the non-crystalline structure. We now call the intergranular glass phase Glass A, and the boundary glass phase Glass B. Fig. 11 shows the transmission micrograph of the layer-like TiN precipitates. The microstructure also consists of the TiN grains (grain size:  $0.5 \sim 1\mu\text{m}$ ) and the boundary glass phase (Glass C). Table 1 indicates the mean chemical compositions of the TiN precipitates and Glasses A, B and C determined by AEM analysis. As illustrated by the values in Table 1, Glasses A and B are made from the components Al-Si-Ca-Ti-Y of the same type, whereas the contents of the main components Al, Si, Ti and Y in Glass A are evidently distinct from those in Glass B. It is well known that the addition of  $\text{Al}_2\text{O}_3$  and/or  $\text{TiO}_2$  tends to enhance immiscibility in complex silicate systems.<sup>9)</sup> Furthermore, a miscibility gap is found in the systems  $\text{SiO}_2\text{-Y}_2\text{O}_3$ <sup>10)</sup> and  $\text{SiO}_2\text{-TiO}_2$ .<sup>11)</sup> Therefore, the formation of Glasses A and B in the oxynitride glassy layer is considered as being a result of the phase separation phenomena. On the other hand, the precipitated TiN slightly contains the impurities Al, Si, Ca and Y, but over 90% of it comes from the component Ti. Glass C is

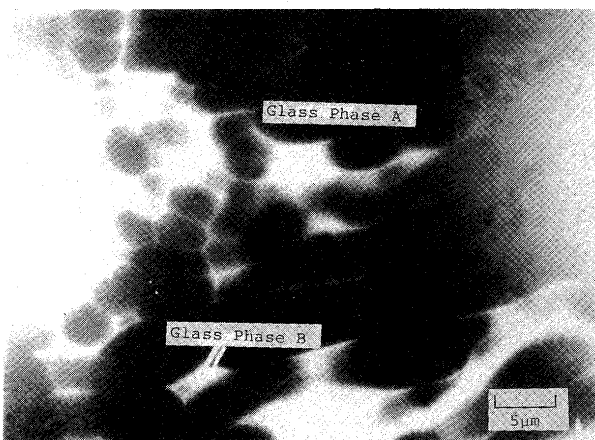


Fig. 10 Transmission micrograph of the oxynitride glassy layer.

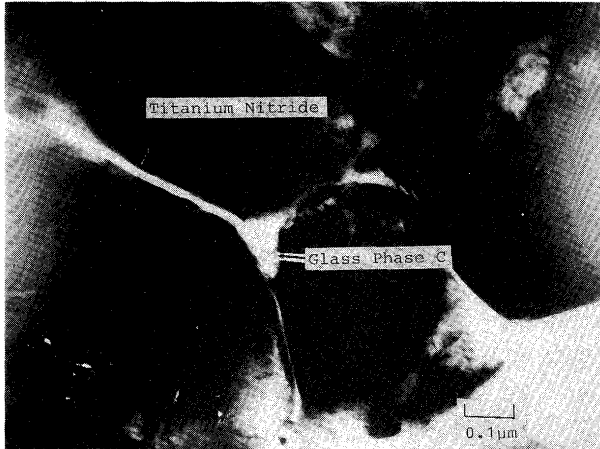


Fig. 11 Transmission micrograph of the layer-like TiN precipitates.

mainly made of Ti-rich  $\text{TiO}_2\text{-SiO}_2$  glass.

### 3.3 Bond strength of $\text{Si}_3\text{N}_4$ joints

We have succeeded in getting  $\text{Si}_3\text{N}_4$  joints with strong bond strength by our joining technique<sup>†</sup>. Table 2 lists the values of the bond strength of the typical  $\text{Si}_3\text{N}_4$  joints at room-temperature measured by a four-point bending test. The bonded  $\text{Si}_3\text{N}_4$  is so strong as to be able to be put to

Table 1 Mean chemical compositions of TiN precipitates and glass phases A, B and C determined by AEM analysis.

Element	TiN precipitate <sup>*1</sup>	Glass A <sup>*2</sup>	Glass B <sup>*3</sup>	Glass C <sup>*4</sup>
Al	2.4	34.5	22.2	4.1
Si	4.2	32.2	36.8	31.4
Ca	1.1	1.6	3.3	6.0
Ti	90.3	10.1	19.2	53.5
Y	2.3	21.3	18.6	4.5
Fe	—	—	—	0.6

Data based on average values of \*1: 7-points; \*2: 10-points; \*3: 5-points; \*4: 7-points.

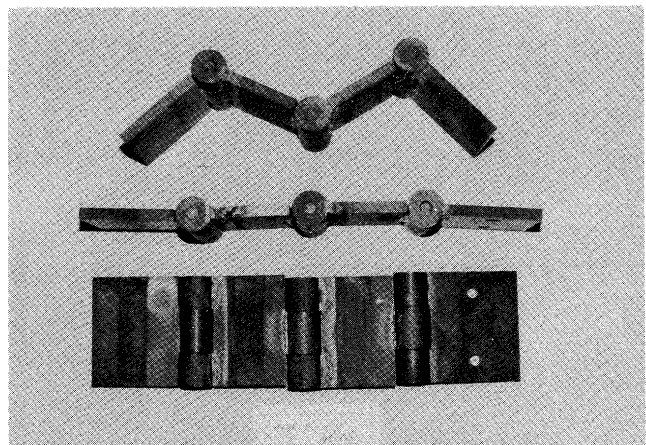


Fig. 12 Curtain for the hot blast stove in steelmaking.

practical use (see Fig. 12).

As illustrated by the values in Table 2, the bond strength increased by the addition of  $\alpha\text{-Si}_3\text{N}_4$  powder to 35wt%CaO-40wt% $\text{SiO}_2$ -25wt% $\text{TiO}_2$  glass solder. By the addition of  $\text{Si}_3\text{N}_4$  powder to the glass solder, the thermal expansion coefficient of the glass is matched closely to that of the  $\text{Si}_3\text{N}_4$  ceramics used. Therefore, the addition of  $\text{Si}_3\text{N}_4$  tends to decrease the residual stress resulting from mismatching, and consequently will lead to a higher bond strength of the  $\text{Si}_3\text{N}_4$  joints. Furthermore, the addition of  $\text{Si}_3\text{N}_4$  tends to accelerate nitridation reactions at the joint region during the joining process.

Table 2 Bond strength (kg/mm<sup>2</sup>) of the  $\text{Si}_3\text{N}_4$  joints<sup>\*1</sup>.

$\alpha\text{-Si}_3\text{N}_4$ <sup>*2</sup>	$\text{N}_2$ -atmosphere 35wt%CaO-40 $\text{SiO}_2$ -25 $\text{TiO}_2$					30CaO-35 $\text{SiO}_2$ - 35 $\text{TiO}_2$ 1	5 kg/cm <sup>2</sup> $\text{N}_2$		
	35wt%CaO-40 $\text{SiO}_2$ -25 $\text{TiO}_2$						35CaO-40 $\text{SiO}_2$ -25 $\text{TiO}_2$		
	0	10	20	30	40wt%		1.	2.	
1.	28.8	27.0	21.1	25.3	26.9	1.	30.5	1.	31.6
2.	25.6	30.3	22.9	23.7	12.5	2.	16.1	2.	20.3
3.	21.6	21.3	38.4	29.4	19.5	3.	14.4	3.	25.9
4.	19.6	18.0	25.3	32.5	20.5	4.	33.4	4.	24.6
Av.	24.0	24.3	26.9	27.7	19.9	Av.	23.6	Av.	25.6 kg/mm <sup>2</sup>

\*1: Reacting at 1500°C × 30 min in each atmosphere.

\*2:  $\alpha\text{-Si}_3\text{N}_4$  powder: particle size 10 μm ≥ 97%;  $\alpha$ -powder ratio ≥ 90%.

<sup>†</sup> The test bars were joined under the following atmospheres:

$\text{N}_2$ ,  $\text{N}_2$  of 5 kg/cm<sup>2</sup>, Ar and 5 $\text{H}_2$ /95 $\text{N}_2$ .

#### 4. Conclusion

Si<sub>3</sub>N<sub>4</sub>-Si<sub>3</sub>N<sub>4</sub> joining was accomplished using glass interface layers in the CaO-SiO<sub>2</sub>-TiO<sub>2</sub> system that reacts with the Si<sub>3</sub>N<sub>4</sub> surface at temperature of 1400°–1600°C under N<sub>2</sub> atmosphere and densified.

Information of the microstructure of the joint region in the bonded Si<sub>3</sub>N<sub>4</sub> was obtained by several microscopic measurements. EPMA observation indicated that the elements Ti and N formed a layer-like titanium nitride compound in the joint region, and that the densification aid elements Al and Y for the Si<sub>3</sub>N<sub>4</sub> ceramics used were densely distributed over all into the joint region by the diffusion from the Si<sub>3</sub>N<sub>4</sub> grain boundaries. The Ti-rich layer-like compound was identified as distorted TiN crystalline by X-ray microdiffraction measurement. SEM-EDX and AEM observations revealed that there was a thin-layer, which consists of a few oxynitride glasses based on Al-Si-Y-Ca-Ti system, between the Si<sub>3</sub>N<sub>4</sub> and TiN precipitates.

We have succeeded in getting the Si<sub>3</sub>N<sub>4</sub> joints with strong bond strength by our joining technique. Furthermore, we confirmed that the bond strength increased by the addition of  $\alpha$ -Si<sub>3</sub>N<sub>4</sub> powder to the CaO-SiO<sub>2</sub>-TiO<sub>2</sub>

glass solder.

#### References

- 1) P. F. Bencher and S. A. Halen: Ceramic Bulletin, **58** (1984), 582.
- 2) R. E. Loehman: J. Non-Cryst. Solids, **42** (1980), 433.
- 3) R. D. Brittain, S. M. Johnson, R. H. Lamoreaux and D. J. Rowcliffe: J. Am. Ceram. Soc., **67** (1984), 522.
- 4) Y. Owada and K. Kobayashi: J. Ceram. Soc. Japan, **92** (1984), 693 (in Japanese).
- 5) R. E. Loehman: Surface and Interfaces in Ceramics and Ceramic-Metal Systems, edited by J. A. Pask and A. G. Evans, Plenum Press, New York, 1981, p. 701–711.
- 6) M. L. Mecartney, R. Sinclair and R. E. Loehman: J. Am. Ceram. Soc., **68** (1985), 472.
- 7) S. M. Johnson and D. J. Rowcliffe: J. Am. Ceram. Soc., **68** (1985), 468.
- 8) N. Iwamoto and N. Umesaki: J. High Temp. Soc., **10** (1984), 132 (in Japanese).
- 9) W. D. Kingery, H. K. Bowen and D. R. Uhlmann: Introduction to Ceramics, John Wiley & Sons, New York, 1975, p. 117–123.
- 10) N. A. Torpov: Trans. Interm. Ceram. Congr., 7th, London, 1960, p. 438.
- 11) R. C. DeVries, R. Roy and E. F. Osborn: Trans. Brit. Ceram. Soc., **53** (1954), 531.